PROCESS DESIGN AND CONTROL

Iterative Identification of Continuous-Time Hammerstein and Wiener Systems Using a Two-Stage Estimation Algorithm

Ho-Tsen Chen, Shyh-Hong Hwang,* and Chuei-Tin Chang

Department of Chemical Engineering, National Cheng Kung University, Tainan, Taiwan 70101, R.O.C.

This article presents an iterative method to deal with the identification of continuous-time single-input/single-output Hammerstein and Wiener systems, characterized by a series connection of a nonlinear static element and a linear dynamic element. The internal variable between the nonlinear and linear elements is inaccessible to measurements so that simultaneous parameter estimation of the two elements cannot be easily achieved in a least-squares fashion. This difficulty could be circumvented by updating the internal variable at each iteration step. A two-stage estimation algorithm, in conjunction with moving-horizon smoothing and a solution-guiding mechanism, is established to ensure the convergence and accuracy of the iterative method in the face of linear structure mismatch, high static nonlinearity with an unknown characteristic, and severe noise. At the first stage, a good description of the static nonlinearity is given by a multisegment function or a polynomial in an iterative manner. Linear structure mismatch is allowed for this stage of estimation. At the second stage, the identification problem is reduced to a simple linear one with the internal variable gained at the first stage. A noniterative procedure can then be applied to determine accurately the structure and parameters of the linear dynamic element. Studies with simulated and experimental examples demonstrate that the proposed identification method is valid for a wide variety of nonlinear system dynamics and test conditions.

1. Introduction

Most chemical or industrial processes are nonlinear and continuous in nature. Identifying such processes as linear models is a mature task,[1,2] but their applications in control techniques will be limited to a narrow operating region. When the operating region becomes wider, the nonlinearity of the process cannot be ignored and hence a control design based on a linear model will be inappropriate. A better alternative is to identify the nonlinear process as a block-oriented model, which consists of a nonlinear static element and a linear dynamic element connected in series.[3] The linear dynamic block can either be preceded or followed by a nonlinear static block, referred to as a Hammerstein and a Wiener system, respectively. Hammerstein and Wiener systems are related very closely to linear ones and can be easily adapted to linear control techniques.[4]

Some nonlinear processes are essentially of Hammerstein or Wiener type, such as a nonlinear flow control valve in cascade with a linear dynamic element[5] and a pH neutralization process involving linear mixing dynamics in a stirred vessel with the pH characterized by a nonlinear static titration curve.[6,7] Moreover, it has been found that Hammerstein or Wiener models may account for nonlinear effects encountered in many chemical and industrial processes, such as exothermic chemical reactors, high-purity distillation columns, furnaces, and heat exchangers.[8−10] Boyd and Chua[11] have proven that any time-invariant process with fading memory can be approximated by a Volterra series representation which in turn can be realized by a Wiener model with polynomial static nonlinearity.

The type and degree of static nonlinearity in a Hammerstein or Wiener system is often unknown. Some nonparametric methods approximate the static nonlinearity by a kernel regression function.[12,13] Although these methods require almost no prior knowledge about the system nonlinearity, the complex forms of the nonlinear estimates make their applications limited in practice.[14] To overcome this problem, many parametric methods adopt a parametrization of the static nonlinearity by a polynomial of finite degree,[15,16] a two-segment polynomial,[17,18] a piecewise linear map,[19−22] or a neural network.[23−25] The construction of such approximations demands knowing certain prior information about the system nonlinearity. If selected improperly, for example, using a polynomial fit for saturation characteristics, the nonlinear approximations might become poor, rendering the simultaneous or subsequent estimation of the linear dynamics erroneous.

A number of identification methods for Hammerstein or Wiener models have been elaborated to separate the identification of the nonlinear static part from that of the linear dynamic part. Inevitably, these methods involve a special design of the test input signal that enables the decoupling of the linear and nonlinear parts. Su and McAvoy[23] proposed to use two sets of test data, steady-state and transient, to identify the nonlinear static and linear dynamic parts of a discrete Hammerstein model, respectively. Sung[26] suggested using a special test signal for continuous-time Hammerstein model identification. Bai[27] and Jia et al.[28] applied the same test signal to identify a discrete Hammerstein model. The test signal is composed from a pseudorandom binary sequence (PRBS) input followed by a random multistep input. Notably, the PRBS input, that shifts between two levels, could excite only the linear dynamic part and hence produce a data set suited to its sole identification. With the linear dynamic part given, the multistep input then excites a data set for the identification of the remaining nonlinear static part. These methods are disadvantageous in that their algorithms cannot adapt to Wiener model identification and the requirements on the specific test signal cause extra implementa-

* To whom correspondence should be addressed. E-mail: shhwang@mail.ncku.edu.tw. Tel.: 886-6-2757575 ext. 62661. Fax: 886-6-2344496.

10.1021/ie800149w CCC: $40.75
Published on Web 01/05/2009

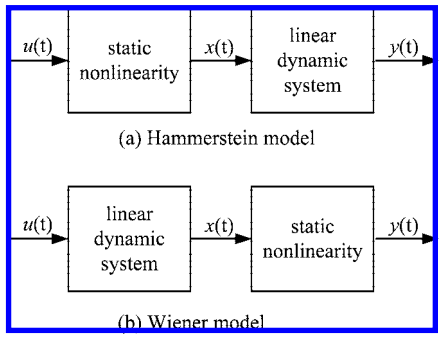

Figure 1. Two classes of block-oriented models.

tion complexity as well as inefficient utilization of the entire test data. Huang et al.[9] presented a method to identify a continuous-time Wiener model using a symmetric relay test input. Lee and Huang[10] extended the method to identify a continuous-time Hammerstein model. Both methods employ an optimization procedure to find an inverse of the static nonlinearity that restores symmetric cycling of the output of the relay test. Once the inverse is obtained, the identification problem is reduced to a linear one and the linear dynamic element can be identified by any available linear technique. Some constraints on the methods are that the nonlinear static element must be invertible, the computation burden is quite heavy, and the identified linear model should be of low order owing to limited information provided by the relay test.

Simultaneous parametric identification of the nonlinear and linear elements for Hammerstein and Wiener systems has the advantages of implementation easiness and efficient utilization of the test data. However, it suffers from the situation that the internal variable between the nonlinear and linear parts is inaccessible to measurements. As a result, the regression equation may not be linear-in-parameters and the conventional least-squares algorithm is not easily applicable. This problem could be circumvented by an iteration procedure with the internal variable updated at each iteration step. The major difficulty is that the convergence of parameter estimates to the actual values is not always warranted due to the coupling between the nonlinear static and linear dynamic parts. The convergence properties are affected by the assumed form of static nonlinearity, degree of nonlinearity, selection of the exciting input, initial guess of the internal variable, linear structure mismatch, and measurement noise.[20,24,27,29,30] Voros[17,18,22] developed several iterative methods to identify discrete Hammerstein and Wiener models, where the static nonlinearity is approximated by a two-segment polynomial or a multisegment piecewise linear function. Using the decomposition technique, the regression equation can be made linear-in-parameters for iterative estimation. Voros's methods will be faced with a serious convergence problem when the structure of the linear element is incorrectly selected, the static nonlinearity cannot be described well by the assumed nonlinear function, or the measured output is corrupted by severe noise.

In this work, an iterative method is presented to identify a continuous-time single-input/single-output (SISO) Hammerstein or Wiener model by approximating the static nonlinearity by an appropriate function and providing effective formulae for updating the internal variable. A two-stage estimation algorithm, incorporating moving-horizon smoothing and a solution-guiding mechanism, is developed to ensure the convergence and accuracy of the iterative method in the face of linear structure mismatch, high static nonlinearity with an unknown characteristic, and severe noise. The first stage of the algorithm arrives

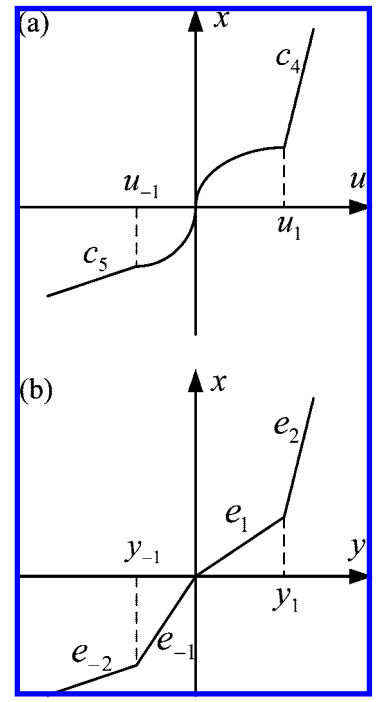

Figure 2. Approximations for static nonlinearity: (a) three-segment function for the Hammerstein model; (b) four-segment inverse function for the Wiener model.

at a good description of static nonlinearity by virtue of a multisegment function or a polynomial in an iterative manner. The second stage of the algorithm reduces the identification problem to a simple linear one with the internal variable acquired previously. A noniterative procedure can then be applied to determine the structure and parameters of the linear dynamic element.

2. Nonlinear SISO System Description for Identification

Here, we consider the identification of continuous-time Hammerstein and Wiener models as depicted in Figure 1. The input and output variables, $u(t)$ and $y(t)$, are measurable. However, the intermediate signal $x(t)$ between the linear dynamic block and the nonlinear static block, called the internal variable, is inaccessible to measurements.

2.1. Identification of Hammerstein Models. As seen in Figure 1a, the linear dynamic element of a Hammerstein model relating $x(t)$ to $y(t)$ can be described by the following differential equation:

$$a_n y^{(n)}(t) + a_{n-1} y^{(n-1)}(t) + \cdots + a_1 y^{(1)}(t) + y(t) = b_m x^{(m)}(t-d) + b_{m-1} x^{(m-1)}(t-d) + \cdots + b_1 x^{(1)}(t-d) + b_0 x(t-d) \quad (1)$$

where a_i and b_i are the model parameters of the linear part, n and m are system orders, d is time delay, and the superscript (j) denotes the jth derivative with respect to time. Moreover, assume that the nonlinear static element relating $u(t)$ to $x(t)$ can be approximated by a polynomial of degree p:

$$x(t) = \sum_{i=1}^{p} c_i [u(t)]^i \quad (2)$$

where c_i are the model parameters of the nonlinear part. Without loss of generality from an input-output viewpoint, we can arbitrarily assign the parameter b_0 to be 1 and allow c_i to account

for the static gain of the nonlinear part. Substituting eq 2 into the $x(t–d)$ term of eq 1 and rearranging the resulting equation gives rise to

$$y(t) = -\sum_{i=1}^{n} a_i y^{(i)}(t) + \sum_{i=1}^{m} b_i x^{(i)}(t-d) + \sum_{i=1}^{p} c_i [u(t-d)]^i \quad (3)$$

In some Hammerstein processes, the static nonlinearity cannot be fitted well by a low-degree polynomial, for example, saturation characteristics in a flow control valve. On the other hand, using a high-degree polynomial would increase the number parameters to be estimated and cause excess errors in the least-squares estimation. We thus replace the polynomial in eq 2 by a three-segment function composed from a cubic polynomial and two straight lines as depicted in Figure 2a. The internal variable $x(t)$ is then given by the three-segment function of $u(t)$ as

$$x(t) = \begin{cases} c_4[u(t) - u_1] + \sum_{j=1}^{3} c_j u_1^j, & \text{if } u(t) \geq u_1 \\ c_1 u(t) + c_2[u(t)]^2 + c_3[u(t)]^3, & \text{if } u_{-1} \leq u(t) < u_1 \\ c_5[u(t) - u_{-1}] + \sum_{j=1}^{3} c_j u_{-1}^j, & \text{if } u(t) < u_{-1} \end{cases} \quad (4)$$

where c_4 and c_5 are the slopes of the two straight lines on both sides, and c_1 through c_3 denote the coefficients of the middle cubic polynomial passing through the chosen steady state ($x = u = 0$). The two partition points (or break points), u_1 and u_{-1}, divide the nonlinear static range of interest into three subregions in terms of $u(t)$.

To convert the above relations (eq 4) into a single expression, we apply the decomposition technique proposed by Voros[17] and define three switching functions $h_i[u(t)]$ as

$$h_1[u(t)] = \begin{cases} 1, & \text{if } u(t) \geq u_1 \\ 0, & \text{otherwise} \end{cases}$$

$$h_0[u(t)] = \begin{cases} 1, & \text{if } u_{-1} \leq u(t) < u_1 \\ 0, & \text{otherwise} \end{cases}$$

$$h_{-1}[u(t)] = \begin{cases} 1, & \text{if } u(t) < u_{-1} \\ 0, & \text{otherwise} \end{cases} \quad (5)$$

Note that each switching function is nonzero only in its specific subregion. It follows that eq 4 can be expressed in more appropriate form:

$$x(t) = \sum_{i=1}^{5} c_i f_i(t) \quad (6)$$

where

$$f_i(t) = [u(t)]^i h_0[u(t)] + u_1^i h_1[u(t)] + u_{-1}^i h_{-1}[u(t)], \quad i = 1, 2, 3$$

$$f_4(t) = [u(t) - u_1] h_1[u(t)]$$

$$f_5(t) = [u(t) - u_{-1}] h_{-1}[u(t)] \quad (7)$$

Substituting eq 6 into the $x(t - d)$ term of eq 1 yields the following regression equation:

$$y(t) = -\sum_{i=1}^{n} a_i y^{(i)}(t) + \sum_{i=1}^{m} b_i x^{(i)}(t-d) + \sum_{i=1}^{5} c_i f_i(t-d) \quad (8)$$

Equations 3 and 8 are two regression equations that are linear-in-parameters provided that $y(t)$, $u(t)$, and $x(t)$ are given. They constitute the underlying equations for the least-squares parameter estimation of a Hammerstein model. Nevertheless, two problems remain to be solved. First, the internal variable $x(t)$ is not measurable and hence unknown a priori. Second, time derivatives of the variables $y(t)$ and $x(t)$ are not available. The first problem is overcome by an iteration procedure, whereas the second problem can be eliminated by applying an integral transform on the differential equation as will be elaborated later.

2.2. Identification of Wiener Models. As seen in Figure 1b, a Wiener model can be described by

$$a_n x^{(n)}(t) + a_{n-1} x^{(n-1)}(t) + \cdots + a_1 x^{(1)}(t) + x(t) = b_m u^{(m)}(t-d) + b_{m-1} u^{(m-1)}(t-d) + \cdots + b_1 u^{(1)}(t-d) + b_0 u(t-d) \quad (9)$$

and

$$y(t) = \sum_{i=1}^{p} c_i [x(t)]^i \quad (10)$$

Equation 9 represents the linear dynamic part with the internal variable $x(t)$ as output, whereas eq 10 approximates the nonlinear static part by a polynomial of $x(t)$. Without loss of generality, we let $c_1 = 1$ and obtain the following expression:

$$x(t) = y(t) - \sum_{i=2}^{p} c_i [x(t)]^i \quad (11)$$

Substituting eq 11 into the $x(t)$ term in eq 9 yields

$$y(t) = -\sum_{i=1}^{n} a_i x^{(i)}(t) + \sum_{i=0}^{m} b_i u^{(i)}(t-d) + \sum_{i=2}^{p} c_i [x(t)]^i \quad (12)$$

The approximation by eq 10 does not require that the static nonlinearity be invertible. However, some Wiener processes, such as a pH neutralization process, consist of severe static nonlinearity whose close approximation demands a high-degree polynomial of $x(t)$. It is found that using a high-degree polynomial of the unknown $x(t)$ would cause a serious convergence problem in the iteration procedure. As a remedy, we assume that the static nonlinearity is invertible and seek a piecewise linear inverse function that calculates $x(t)$ according to the measured output $y(t)$. For better convergence, a four-segment piecewise linear function is established as

$$x(t) = \begin{cases} e_2[y(t) - y_1] + e_1 y_1, & \text{if } y(t) \geq y_1 \\ e_1 y(t), & \text{if } 0 \leq y(t) < y_1 \\ e_{-1} y(t), & \text{if } y_{-1} \leq y(t) < 0 \\ e_{-2}[y(t) - y_{-1}] + e_{-1} y_{-1}, & \text{if } y(t) < y_{-1} \end{cases} \quad (13)$$

where e_i denote the slopes of the four linear segments. The function is defined on an interval of $y(t)$ as depicted in Figure 2b, which is partitioned into four subintervals with three break points, y_1, 0, and y_{-1}. The use of the four-segment piecewise linear function could greatly improve the convergence properties of the iteration procedure by mitigating the coupling between the nonlinear and linear parts. On the contrary, this coupling would become rather significant if the nonlinear function is defined over the internal variable $x(t)$ as in eq 10, which will vary widely with the iterative estimation of the linear dynamic part. Consequently, the use of eq 13 could result in better convergence properties for a wider range of test data (or higher nonlinearity) than the use of eq 10.

Using the decomposition technique, we define four switching functions $h_i[y(t)]$:

$$h_2[y(t)] = \begin{cases} 1, & \text{if } y(t) \geq y_1 \\ 0, & \text{otherwise} \end{cases}$$

$$h_2[y(t)] = \begin{cases} 1, & \text{if } 0 \leq y(t) < y_1 \\ 0, & \text{otherwise} \end{cases}$$

$$h_{-1}[y(t)] = \begin{cases} 1, & \text{if } y_{-1} \le y(t) < 0 \\ 0, & \text{otherwise} \end{cases}$$

$$h_{-2}[y(t)] = \begin{cases} 1, & \text{if } y(t) < y_{-1} \\ 0, & \text{otherwise} \end{cases} \quad (14)$$

Without loss of generality, we can let $e_1 = 1$ and reformulate eqs 13 and 14 to yield

$$x(t) = y(t) - \sum_{i=-2;i\neq 0,1}^{2} (1 - e_i)\, g_i(t) \quad (15)$$

where

$$g_{-2}(t) = [y(t) - y_{-1}]h_{-2}[y(t)]$$
$$g_{-1}(t) = y(t)h_{-1}[y(t)] + y_{-1}h_{-2}[y(t)]$$
$$g_2(t) = [y(t) - y_1]h_2[y(t)] \quad (16)$$

Substituting eq 15 into the $x(t)$ term in eq 9 gives rise to

$$y(t) = -\sum_{i=1}^{n} a_i x^{(i)}(t) + \sum_{i=0}^{m} b_i u^{(i)}(t-d) + \sum_{i=-2;i\neq 0,1}^{2} (1 - e_i)\, g_i(t) \quad (17)$$

Equations 12 and 17 constitute the underlying regression equations for the identification of a Wiener model. They are both linear-in-parameters if $x(t)$ is updated at each iteration step.

3. Time-Weighted Integral Transform

To deal with the time derivatives in the foregoing regression equations, which are never available in practice, we extend the time-weighted integral transform proposed by Hwang and Lin[2] for linear systems to nonlinear Hammerstein and Wiener systems. They defined an lth-order integral transform to convert a continuous-time signal $f(t)$ over a time interval $[t_a, t_b]$ into a real number:

$$T_l\{f(t)\} = \int_{t_a}^{t_b} w^{(l)}(t)\, f(t)\, \mathrm{d}t \quad (18)$$

where $w(t)$ is the weighting function. The zeroth-order transform for the ith derivative of the signal, $f^{(i)}(t)$, can be derived as

$$T_0\{f^{(i)}(t)\} = \int_{t_a}^{t_b} w(t)\, f^{(i)}(t)\, \mathrm{d}t, \quad i = 1, 2, \cdots, n \quad =$$
$$(-1)^i T_i\{f(t)\} + \sum_{j=0}^{i-1} (-1)^j \left[w^{(j)}(t_b) f^{(i-1-j)}(t_b) - w^{(j)}(t_a) f^{(i-1-j)}(t_a) \right] \quad (19)$$

The above formula results from repetitive use of integration by parts, giving rise to the infeasible summation term that involves various time derivatives of the signal at t_a and t_b. To avoid its evaluation, the weighting function is chosen as

$$w(t) = (t - t_a)^n (t - t_b)^n \quad (20)$$

such that

$$w^{(n-1)}(t_a) = w^{(n-2)}(t_a) = \cdots = w(t_a) = 0$$
$$w^{(n-1)}(t_b) = w^{(n-2)}(t_b) = \cdots = w(t_b) = 0$$

It is apparent that for $i \le n$, the summation term in eq 19 is eliminated by incorporating the specific form of $w(t)$. As a result, eq 19 reduces to

$$T_0\{f^{(i)}(t)\} = (-1)^i T_i\{f(t)\}, \quad i = 0, 1, \cdots, n \quad (21)$$

Taking the zeroth-order transform on both sides of eq 8 and applying eq 21 with $f(t)$ replaced by $y(t)$, $x(t)$, or $f_i(t)$ yields a new regression equation for the Hammerstein model:

$$T_0\{y(t)\} = \boldsymbol{\varphi}_h(t_a, t_b)^T \boldsymbol{\theta}_h \quad (22)$$

where the regression vector $\boldsymbol{\varphi}_h$ and the parameter vector $\boldsymbol{\theta}_h$ are given by

$$\boldsymbol{\varphi}_h(t_a, t_b)^T = [(-1)^{n-1} T_n\{y(t)\} \cdots T_1\{y(t)\} \quad (-1)^m T_m\{x(t-d)\} \cdots -T_1\{x(t-d)\} \quad T_0\{f_1(t-d)\} \cdots T_0\{f_5(t-d)\}]$$

$$\boldsymbol{\theta}_h = [a_n \cdots a_1 \quad b_m \cdots b_1 \quad c_1 \cdots c_5]^T$$

Using eq 21 with $f(t)$ replaced by $y(t)$, $x(t)$, $u(t)$, or $g_i(t)$, we derive a new regression equation for the Wiener model from eq 17 as

$$T_0\{y(t)\} = \boldsymbol{\varphi}_w(t_a, t_b)^T \boldsymbol{\theta}_w \quad (23)$$

where the regression vector $\boldsymbol{\varphi}_w$ and the parameter vector $\boldsymbol{\theta}_w$ are given by

$$\boldsymbol{\varphi}_w(t_a, t_b)^T = [(-1)^{n-1} T_n\{x(t)\} \cdots T_1\{x(t)\} \quad (-1)^m T_m\{u(t-d)\} \cdots T_0\{u(t-d)\} \quad T_0\{g_{-2}(t)\} \quad T_0\{g_{-1}(t)\} \quad T_0\{g_2(t)\}]$$

$$\boldsymbol{\theta}_w = [a_n \cdots a_1 \quad b_m \cdots b_0 \quad 1 - e_{-2} \quad 1 - e_{-1} \quad 1 - e_2]^T$$

4. Iterative Identification Method with a Two-Stage Estimation Algorithm

In this section, an iterative identification method for Hammerstein and Wiener models is developed based on the two regression equations (eqs 22 and 23) derived according to the approximations by the multisegment functions. If a polynomial function is preferred (e.g., the static nonlinearity is not invertible for Wiener identification), the corresponding regression equation can be derived by taking the zeroth-order transform on eq 3 or 12. It will be shown, however, that the use of the multisegment functions is more reliable for the sake of convergence and accuracy subject to higher static nonlinearity.

4.1. Moving-Horizon Least-Squares Estimators. Note that eqs 22 and 23 are dependent upon two arguments, t_a and t_b. Therefore, insofar as sufficient data of $u(t)$, $x(t)$, and $y(t)$ are available, one can generate a preferred number of linear regression relations by choosing different sets of time intervals (or moving horizons) for the integral transform. For instance, the kth regression relation can be created by performing the integration over a time horizon between $t_a(k)$ and $t_b(k)$. The following formulae are recommended to produce N regression relations for subsequent least-squares estimation:

$$t_a(k) = t_0 + \lambda(k-1)\eta, \quad t_b(k) = t_a(k) + \eta, \quad k = 1, 2, \cdots, N \quad (24)$$

where t_0 and t_f ($= t_a(N) + \eta$) denote, respectively, the initial time and final time for data acquisition. Each time horizon starts from a different $t_a(k)$ and has the same horizon length η. The least-squares estimator for the Hammerstein model, $\hat{\boldsymbol{\theta}}_h$, is then given by

$$\hat{\boldsymbol{\theta}}_h = \left[\sum_{k=1}^{N} \boldsymbol{\varphi}_h(k)\, \boldsymbol{\varphi}_h(k)^T \right]^{-1} \sum_{k=1}^{N} \left[\boldsymbol{\varphi}_h(k) \int_{t_a(k)}^{t_b(k)} w(t)\, y(t)\, \mathrm{d}t \right] \quad (25)$$

and that for the Wiener model, $\hat{\boldsymbol{\theta}}_w$, can be calculated as

$$\hat{\boldsymbol{\theta}}_w = \left[\sum_{k=1}^{N} \boldsymbol{\varphi}_w(k) \boldsymbol{\varphi}_w(k)^T \right]^{-1} \sum_{k=1}^{N} \left[\boldsymbol{\varphi}_w(k) \int_{t_a(k)}^{t_b(k)} w(t)\, y(t)\, \mathrm{d}t \right] \quad (26)$$

The least-squares estimators require three arguments, η, λ, and N, to be set a priori. The arguments λ and N are determined by the computation capacity and total data available, which are not crucial to estimation accuracy. A number between 0.05 and 0.2 can be chosen for λ. However, the horizon length η should be given a sufficiently large value to ensure the convergence of the estimator at the first stage estimation of the algorithm as will be elaborated later. It is suggested that η for the first stage estimation be set between one and two times the process settling time (95% response time).

4.2. Iteration Procedure Based on Updating the Internal Variable. The calculation of the two estimators (eqs 25 and 26) demands knowing the internal variable $x(t)$. Though not measurable, its estimate can be provided with a prescribed updating formula at each iteration step. For the Hammerstein model, it is natural to employ eq 6 describing the nonlinear static part to compute $x(t)$ at the $(k+1)$th step as

$$\hat{x}(t;k+1) = \sum_{i=1}^{5} \hat{c}_i(k)\, f_i(t) \tag{27}$$

where $\hat{c}_i(k)$ denotes the parameter estimates of c_i at the kth step. It is not suited to calculate $x(t)$ from the estimated linear dynamic block because it demands the inversion of the linear block, which is usually nonexistent.

For the Wiener model with an invertible nonlinear static part, there are two formulae available for updating the internal variable. The first is obtained by passing the test input $u(t)$ through the estimated linear dynamic block, that is,

$$\hat{x}_{\mathrm{lin}}(t;k+1) = L^{-1}\left\{ \frac{U(s)\, \mathrm{e}^{-ds} \sum_{i=0}^{m} \hat{b}_i(k)\, s^i}{1 + \sum_{i=1}^{n} \hat{a}_i(k)\, s^i} \right\} \tag{28a}$$

The second can be calculated according to the approximate inverse of the nonlinear static block given by eq 15 as

$$\hat{x}_{\mathrm{nl}}(t;k+1) = y(t) - \sum_{i=-2;i\neq 0,1}^{2} [1 - \hat{e}_i(k)] g_i(t) \tag{28b}$$

In the above formulae, $\hat{x}_{\mathrm{lin}}(t;k+1)$ and $\hat{x}_{\mathrm{nl}}(t;k+1)$ are two estimates of $x(t)$ at the $(k+1)$th iteration step, $\hat{a}_i(k)$, $\hat{b}_i(k)$, and $\hat{e}_i(k)$ are model parameter estimated at the kth step, L^{-1} denotes the inverse Laplace transform, and $U(s)$ is the Laplace transform of $u(t)$.

It is postulated that if the iteration procedure for the Wiener model does converge to the accurate parameter estimates, the two estimates calculated by eqs 28a and 28b must be identical or at least close to each other. However, with the sole use of eq 28a or 28b, the iteration procedure is likely to converge to an inaccurate solution such that the two estimates of $x(t)$ become widely different. A better alternative for updating $x(t)$ is then to use a hybrid estimate given by

$$\hat{x}(t;k+1) = 0.5\hat{x}_{\mathrm{lin}}(t;k+1) + 0.5\hat{x}_{\mathrm{nl}}(t;k+1) \tag{29}$$

This formula for $x(t)$ takes account of its forward estimate according to $u(t)$ and its backward estimate according to $y(t)$ equally, and hence guides the iteration procedure toward an accurate solution that ensures the consistency of the two $x(t)$ estimates.

We thus propose an iteration procedure for Hammerstein and Wiener models as follows. The procedure is started by the least-squares parameter estimator of eq 25 or 26 with an initial guess of the internal variable $x(t)$. A convenient guess is the supplied input $u(t)$ for the Hammerstein model and the measured output $y(t)$ for the Wiener model. The internal variable $x(t)$ is updated using eq 27 for the Hammerstein model and eq 29 for the Wiener model. The procedure is repeated until the estimator converges.

4.3. Convergence and Accuracy Issues. Two critical issues arise to evaluate the proposed iteration procedure. That is, it must ensure not only the convergence to a single solution but also the accuracy of that solution. Two mechanisms are developed to deal with these issues. The first mechanism is moving-horizon smoothing resulting from the selection of horizon length η. It follows from eqs 18 and 24 that the role of η is to smooth the data within each specified time horizon. This could diminish the effect of noise on parameter estimation. Furthermore, a larger value of η tends to capture more low frequency (large time scale) information from test input−output data, thus favoring the accurate estimation of the nonlinear static part. This allows the iteration procedure to cope properly with the difficulties of linear structure mismatch, high or peculiar static nonlinearity, and severe noise. By linear structure mismatch, we mean that the assumed orders and delay of the linear dynamic part, that is, n, m, and d, may be incorrect. Because the correct linear structure is usually unknown a priori, this mechanism is practically helpful to the accurate approximation of the static nonlinearity.

In the present identification framework for a Hammerstein model, the iteration procedure with the choice of a sufficiently large η would at least guarantee the convergence of the least-squares estimator as well as the estimation accuracy of the static nonlinearity. For the identification of a Wiener model, the convergence problem becomes more stringent and the smoothing mechanism with a higher η does not suffice to ensure the convergence of the estimator to the actual values. Such a situation is often encountered when the range of test data is wide so that the static nonlinearity becomes high. A plausible reason is that the internal variable $x(t)$ may vary widely with the iterative estimation of the linear dynamic part, thus strengthening the coupling between the nonlinear and linear parts especially in the presence of linear structure mismatch. An extra mechanism based on the hybrid $x(t)$ estimate of eq 29 was recommended previously to guide the iteration procedure toward the accurate solution that enhances the consistency of the two $x(t)$ estimates. With the smoothing and solution-guiding mechanisms, the iteration procedure for the Wiener model would also guarantee the convergence of the least-squares estimator as well as the estimation accuracy of the static nonlinearity.

4.4. Two-Stage Estimation Algorithm. As mentioned previously, a larger η would render the approximation of the nonlinear static element more accurate despite linear structure mismatch. This implies that the converged estimate of the internal variable $x(t)$ is also reliable. Conversely, the estimation accuracy of the linear dynamic element is somewhat sacrificed because much of high frequency information (small time scale) about test data has been lost. Some remedy should be applied to recover the estimation accuracy of the linear dynamic part.

Another problem is that the iteration procedure requires knowing the partition points a priori (this is not the case if a polynomial is assumed). Although they are usually unknown in practice, a rough estimate of the partition points can be inferred from the range of test data. We then recommend a two-stage estimation algorithm as follows:

Stage 1. Given the partition points (u_1, u_{-1} or y_1, y_{-1}), apply the iteration procedure with a sufficiently large η to test data. The linear structure (n, m, d) can be quite arbitrarily assumed

at this stage and hence it might be incorrect. To ensure convergence and accuracy, it is suggested to set the η value larger than the process settling time. If the settling time is unknown, one can try different (from small to large) values of η until rather consistent solutions become obtainable. The previous analysis implies that insofar as the selected partition points are appropriate, the identified nonlinear static part and the associated estimate of the internal variable $x(t)$ can be deemed reliable.

Stage 2. Determine the accurate linear structure and estimate the model parameters of the linear dynamic part based on $x(t)$ gained at stage 1. Note that with the reliable estimation of the internal variable, the identification problem can be reduced to a simple linear one, for which a noniterative procedure is able to arrive at more accurate parameter estimates for the linear dynamic part. The method of Hwang and Lin[2] for linear systems can be modified in a trivial way to deal with the resulting linear identification problem. This method includes determination of the linear model structure and estimation of the associated model parameters. For the Hammerstein model, we consider eq 1 with $b_0 = 1$, for which the internal variable $x(t)$ is replaced by that calculated according to eq 27 at stage 1. For the Wiener model, we consider eq 9 with b_0 estimated at stage 1, for which $x(t)$ is replaced by that calculated according to eq 28b. Because that calculated by eq 28a contains no new information about the linear dynamic element, it is not needed in the linear identification problem at this stage. To facilitate the estimation accuracy of the linear dynamic element, a smaller η value should be used. We suggest setting the η value equal to half the settling time for the Hammerstein model and equal to the settling time for the Wiener model. Here, a good estimate of the settling time is obtainable from the linear dynamic element given at stage 1.

5. Determination of Partition Points

The preceding two-stage estimation algorithm relies on an appropriate prior selection of partition points. If such information is not available, a technique is developed to find the optimal partition points. We first consider the Hammerstein case. It is known that the partition points u_1 and u_{-1} must lie within the range of the test input $u(t)$. Assume that this range has an upper bound u_U (>0) and a lower bound u_L (<0). Then the optimal partition points are obtained by finding $u_1 \in [0, u_U]$ and $u_{-1} \in [u_L, 0]$ such that the following prediction error criterion is minimized:

$$J_h(u_1, u_{-1}) = \sum_{k=1}^{N} \left[\int_{t_a(k)}^{t_b(k)} w(t)\, y(t)\, dt - \boldsymbol{\varphi}_h(k)^T \hat{\boldsymbol{\theta}}_h \right]^2 \qquad (30)$$

where $\hat{\boldsymbol{\theta}}_h$ is the least-squares estimator of eq 25 for a selected set of u_1 and u_{-1}.

As for the Wiener case, the partition points y_1 and y_{-1} must lie within the range of the output $y(t)$ with an upper bound y_U (>0) and a lower bound y_L (<0). It is found that the error criterion in a similar form of eq 30 is not sensitive enough to detect the best partition points especially under noisy conditions. A better alternative is to seek $y_1 \in [0, y_U]$ and $y_{-1} \in [y_L, 0]$ such that the following output error criterion is minimized:

$$J_w(y_1, y_{-1}) = \int_{t_0}^{t_f} [y(t) - y_M(t)]^2 \qquad (31)$$

where the predicted output $y_M(t)$ is obtained by passing $\hat{x}_{lin}(t)$, the output of the identified linear dynamic element according to eq 28a, through the identified nonlinear static element as

$$y_M(t) = \begin{cases} [\hat{x}_{lin}(t) - y_1]/\hat{e}_2 + y_1, & \text{if } \hat{x}_{lin}(t) \ge y_1 \\ \hat{x}_{lin}(t), & \text{if } 0 \le \hat{x}_{lin}(t) < y_1 \\ \hat{x}_{lin}(t)/\hat{e}_{-1}, & \text{if } \hat{e}_{-1} y_{-1} \le \hat{x}_{lin}(t) < 0 \\ [\hat{x}_{lin}(t) - \hat{e}_{-1} y_{-1}]/\hat{e}_{-2} + y_{-1}, & \text{if } \hat{x}_{lin}(t) < \hat{e}_{-1} y_{-1} \end{cases} \qquad (32)$$

Recall that the prime requirement of the iteration procedure is to ensure the consistency of $\hat{x}_{lin}(t)$ and $\hat{x}_{nl}(t)$. The criterion of eq 31 means that the measured output $y(t)$, caused by $\hat{x}_{nl}(t)$, and the predicted output $y_M(t)$, caused by $\hat{x}_{lin}(t)$, should be as close as possible.

Supposing the best partition points and the exact linear structure are both unknown, the two-stage estimation algorithm is modified as follows:

Hammerstein Model. First provide a guess of the linear structure (n, m, d) and apply the two-stage algorithm on the basis of the polynomial approximation of eq 2 to find the linear structure. With the newly determined linear structure, apply repetitively the first stage of the algorithm to search for the best partition points, $u_1 \in [0, u_U]$ and $u_{-1} \in [u_L, 0]$, that minimizes the criterion of eq 30. Next according to the estimated internal variable $\hat{x}(t)$ resulting from eq 27, apply the second stage of the algorithm to find the linear structure and then give the linear parameter estimates. This search for the partition points can be repeated until the estimated linear structure converges. Usually a single search would suffice.

Wiener Model. With a guess of the linear structure, apply repetitively the first stage of the algorithm to search for the best partition points, $y_1 \in [0, y_U]$ and $y_{-1} \in [y_L, 0]$, that minimizes the criterion of eq 31. Then according to the estimated internal variable, apply the second stage of the algorithm to infer the linear structure and the corresponding linear parameter estimates. Note that the estimated internal variable is referred to as $\hat{x}_{nl}(t)$ of eq 28b resulting from the best set of y_1 and y_{-1}. With the newly determined linear structure, conduct another search for the best partition points. Usually this second search would arrive at an accurate model. The second search can be avoided if the initial selection of the linear structure is already desirable. For example, the exact linear model structure is given or a model of reduced order is preferred.

6. Simulated and Experimental Examples

Five simulated mathematical and physical examples as well as one experimental real example have been employed to demonstrate the effectiveness of the proposed iterative method in conjunction with the two-stage estimation algorithm. Test data for the simulated examples were generated by zero-mean white random signals with standard deviation σ. The test input was stepwise continuous with switching time T_s and was limited to a range selected so as to make the identification test feasible. To simulate noisy situations, measurement noise was added to corrupt the output data of each test run with the noise-to-signal ratio (NSR) defined as the standard deviation of the noise divided by the standard deviation of the measured output.

Example 1.

$$3y^{(3)}(t) + 4y^{(2)}(t) + 4y^{(1)}(t) + y(t) = -x^{(1)}(t-2) + x(t-2)$$

$$\text{static nonlinearity of type I:} \quad x(t) = \frac{u(t)}{\sqrt{0.1 + 0.9[u(t)]^2}}$$

$$\text{static nonlinearity of type II:} \quad x(t) = -[u(t)]^2 \times [1 - e^{0.7u(t)}]$$

This contrived Hammerstein process comprises a third-order underdamped linear dynamic element preceded by either of the

Table 1. Two-Stage Estimation Results of Example 1

		a_3	a_2	a_1	b_2	b_1	$\overline{\text{VIF}}$	$\text{VIF}_{\max}$
Type I Static Nonlinearity								
case A ($\eta = 15$, $\lambda = 0.1$, $N = 55$)	stage 1	0	7.176	3.702	0	0	60.93	228.0
	stage 2	2.910	3.523	3.715	0	−0.862	1.50	1.79
case B ($\eta = 15$, $\lambda = 0.1$, $N = 55$, $u_1 = 0.5$, $u_{-1} = -0.5$)	stage 1	2.689	4.023	3.869	0	−1.038	46.22	167.2
	stage 2	2.941	4.008	3.930	0	−1.010	1.47	1.85
case C ($\eta = 10$, $\lambda = 0.2$, $N = 43$, $u_1 = 0.5$, $u_{-1} = -0.5$)	stage 1	2.695	3.972	3.870	0.032	−1.039	30.98	93.06
	stage 2	2.950	4.008	3.938	0	−1.008	1.45	1.08
Type II Static Nonlinearity								
case A ($\eta = 15$, $\lambda = 0.1$, $N = 55$)	stage 1	0	6.438	3.669	0	0	58.89	229.7
	stage 2	2.799	3.879	3.652	0	−0.923	1.94	2.52
case B ($\eta = 15$, $\lambda = 0.1$, $N = 55$, $u_1 = 1.8$, $u_{-1} = -0.8$)	stage 1	3.164	4.021	4.109	0	−1.033	25.19	113.6
	stage 2	3.078	4.087	4.082	0	−1.010	1.97	2.65
case C ($\eta = 10$, $\lambda = 0.2$, $N = 43$, $u_1 = 1.8$, $u_{-1} = -0.8$)	stage 1	3.268	4.204	4.124	−0.076	−0.985	22.61	71.17
	stage 2	3.056	4.077	4.049	0	−1.009	1.97	2.56

above nonlinear static elements with distinct characteristics. The linear element has a settling time of about 10. The first nonlinearity, employed by Wigren,[20] simulates a saturation characteristic, while the second nonlinearity, employed by Voros,[17] is like a kind of dead-zone. For Hammerstein identification subject to each type of nonlinearity, test data with NSR = 10% were collected before $t_f = 100$. The random input signals were characterized by $T_s = 1$, $\sigma = 1.25$, and limits of $\pm 2\sigma$.

Table 1 depicts the two-stage identification results as well as the first stage settings of η, λ, and N for three different cases (A−C), assuming that the delay d is known. The first stage settings are quite arbitrarily given so as to meet the data length of $t_f = 100$. At the first stage of case A, a polynomial of degree 5 is employed to approximate the nonlinear static behavior, and a rather incorrect linear structure of $n = 2$ and $m = 0$ is assumed a priori. At the first stages of cases B and C, the three-segment function of eq 4 is chosen, and the partition points u_1 and u_{-1} are determined by a search for the best set. The linear structure inferred by case A is adopted for case B, whereas a different linear structure of $n = 3$ and $m = 2$ is assumed for case C. At the second stage of the algorithm, η is reduced to half the settling time estimated at the first stage and N is increased accordingly to recover the estimation accuracy of the linear dynamic element.

Figure 3 panels a and c reveal that the accurate linear structure ($n = 3$, $m = 1$) is obtainable from the second stage estimation of case A. Note that for each type of static nonlinearity, the error function defined by the method of Hwang and Lin[2] ceases to decrease significantly for $n = 3$ and $m = 1$ (as indicated by an arrow). For case B, the optimal partition points are found by minimizing the criterion of eq 30 as depicted in Figure 3b,d. As a result, the two distinct nonlinear static elements are fitted well as seen in Figure 4, and the parameters of the linear dynamic element are almost exactly estimated by stage 2 as enumerated in Table 1. On the other hand, the identified models are less accurate for case A because of the inadequacy of using a polynomial approximation. In cases B and C, the proposed two-stage algorithm yields equally good Hammerstein models, implying that the algorithm is sensitive to neither the prior assumption of the linear structure nor the first stage settings of η, λ, and N.

Figure 5 compares the convergence and accuracy properties of the proposed iterative method against Voros's Hammerstein method[17] for the process with the saturation nonlinearity. Since both methods assume approximations for the static nonlinearity, it is convenient to evaluate their convergence and accuracy by virtue of the linear parameter estimation with the exact linear structure given. For a fair comparison with Voros's method that deals with a discrete-time linear part, our continuous-time parameter estimates, $\hat{a}_i$ and $\hat{b}_i$, are converted to their discrete-time equivalents, $\hat{a}_i'$ and $\hat{b}_i'$. The accuracy of the linear parameter estimates are then evaluated by

$$\text{percent error of linear parameter estimates} = \frac{\sum_{i=1}^{n} |\hat{a}'_i - a'_i| + \sum_{i=1}^{n} |\hat{b}'_i - b'_i|}{\sum_{i=1}^{n} |a'_i| + \sum_{i=1}^{n} |b'_i|} \times 100$$

The proposed iterative method based on the three-segment function or a polynomial of degree 5 is applied to the foregoing test data with the settings of $\eta = 0.5$, $\lambda = 0.1$, $N = 185$, and $u_{\pm 1} = \pm 0.5$. Note that without linear structure mismatch, it is possible to use a smaller horizon length η to guarantee the accuracy of both the linear and nonlinear parts. Consequently, the second stage of the estimation algorithm is not required here. As expected, the proposed iterative method based on the three-segment function converges very rapidly to the actual solution as shown in Figure 5, whereas the method based on a polynomial converges to a less accurate yet satisfactory solution. Voros's method, however, yields rather erroneous parameter estimates for the linear dynamic part, causing also a failure in approximating well the static nonlinearity as shown in Figure 4a. Similar results are observed for the type II static nonlinearity as seen in Figure 4b.

Example 2.

$$2x^{(3)}(t) + 5x^{(2)}(t) + 4x^{(1)}(t) + x(t) = -2u^{(1)}(t-1) + u(t-1)$$

static nonlinearity of type III: $y(t) =$

$$\begin{cases} \dfrac{x(t)}{\sqrt{0.1 + 0.9[x(t)]^2}} & \text{if } x(t) \geq 0 \\ -[x(t)]^2 \times [1 - e^{0.7x(t)}] & \text{if } x(t) < 0 \end{cases}$$

static nonlinearity of type IV: $y(t) = \dfrac{x(t)}{\sqrt{D + 0.9[x(t)]^2}}$

This contrived Wiener process is composed from a third-order overdamped linear dynamic element followed by either of the above nonlinear static elements. The process has a settling time of about 10. The static nonlinearity of type III, employed by Voros,[18] exhibits distinct features for positive and negative

ranges of $x(t)$. For Wiener identification subject to this type of nonlinearity, test data with NSR = 10% were collected before $t_f = 120$. Four different cases (D−G) using random input signals with limits of ±3 were considered. The input signals were specified as $T_s = 1$ and $\sigma = 1.5$ for cases D and E and as $T_s = 4$ and $\sigma = 0.75$ for cases F and G.

Table 2 lists the two-stage identification results as well as the first stage settings of η, λ, and N, assuming that the delay d is known. The first stage settings are arbitrarily given so as to meet the data length of $t_f = 120$. At the first stages of all cases, the four-segment piecewise linear function defined by eq 13 is adopted with the partition points y_1 and y_{-1} determined appropriately. For case D, an incorrect linear structure of $n = 2$ and $m = 1$ is assumed a priori, whereas for the other cases, the linear structure inferred by case D is employed. At the second stage of the algorithm, η is reduced to the settling time estimated at the first stage and N is increased accordingly to recover the estimation accuracy of the linear dynamic element. In cases F and G, test data are rounded to hundredths to check the adequacy of least-squares solutions involving matrix inversion.

Figures 6a and 6b indicate that for case D, the partition points can be found by minimizing the criterion of eq 31 from the first stage estimation and the accurate linear structure ($n = 3$, $m = 1$) is obtainable from the second stage estimation. With the exact linear structure given, new partition points can be obtained for case E in Figure 6c, leading to better estimation of the linear part as illustrated in Table 2. The static nonlinearity, however, is fitted well for both cases because of the use of a sufficiently large η as evidenced in Figure 7. Figure 6d shows that the prior assumption of the linear structure can be confirmed by the second stage estimation of case E.

Here, we are interested in knowing whether the two-stage algorithm is sensitive to rounding or truncating of test data. It gives an indication of the accuracy of the parameter estimates from matrix inversion. Recall that the test data in cases F and G were rounded to hundredths. The good results seen in Table 2 and Figure 7 indicate that our algorithm is not sensitive to roundoff errors in the test data and those matrices inverted in intermediate least-squares calculations are well-conditioned. Moreover, comparable identification results among the last three cases imply that our algorithm is not sensitive to the switching time of the random input signal and the first stage settings of η, λ, and N.

Figure 8 compares the convergence properties of the proposed iterative method against Voros's Wiener method[18] for the process with the type III nonlinearity. The proposed iterative method based on the four-segment function is applied to the foregoing test data with the setting of $\eta = 10$. With the linear structure given exactly, this η ensures the accuracy of both the linear and nonlinear parts. Consequently, the first stage of the estimation algorithm converges to the actual parameter estimates of the linear part. The slow convergence is because of severe measurement noise. Voros's method, on the other hand, would cause an oscillation between two incorrect solutions.

The constant D in the type IV static nonlinearity can be used to adjust the degree of nonlinearity. Figure 9a reveals that the smaller the constant D is, the higher the static nonlinearity becomes. For a given D, the degree of nonlinearity would also increase with the range of the input test data, namely the

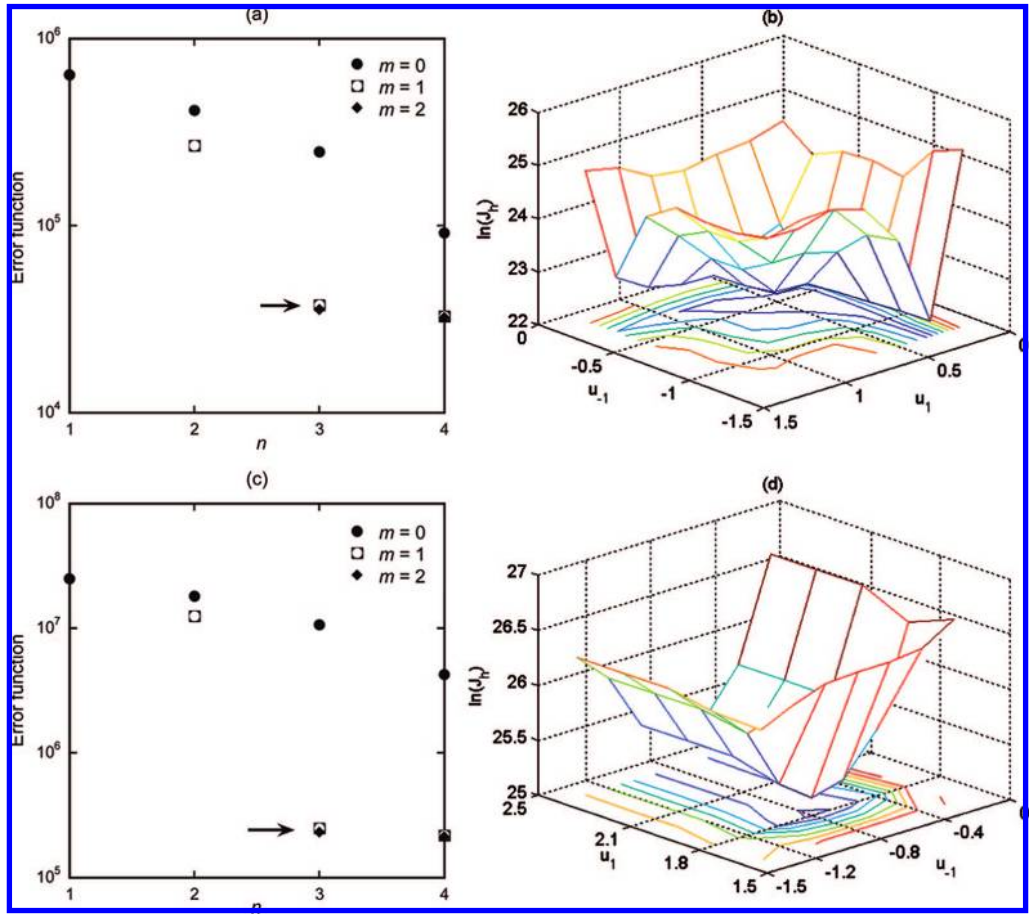

Figure 3. Determination of the linear structure (case A) and partition points (case B) for Hammerstein identification of Example 1: (a, b) type I static nonlinearity; (c, d) type II static nonlinearity.

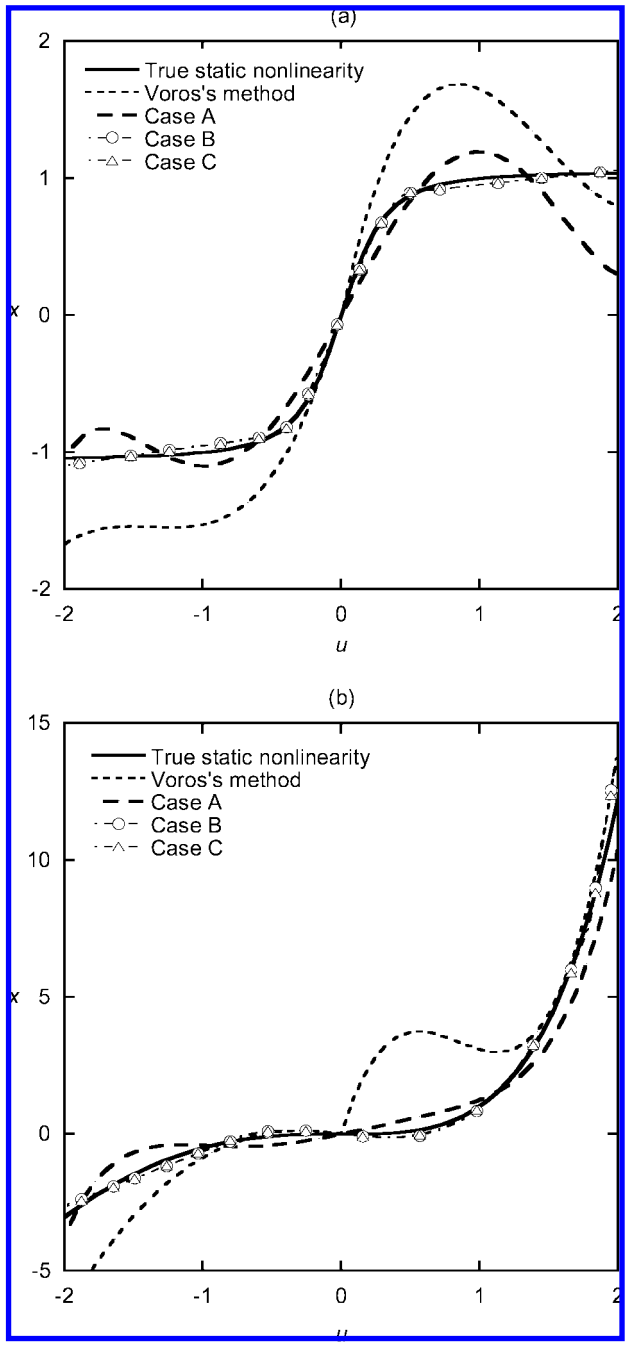

Figure 4. Various approximations of static nonlinearity by Hammerstein identification of Example 1: (a) type I; (b) type II.

standard deviation σ. It is interesting to analyze the convergence and accuracy properties of the proposed iterative method in the face of varying degree of nonlinearity. For this purpose, we assume the exact linear structure and apply the iterative method to noise-free test data with the settings of $\eta = 10$, $\lambda = 0.1$, and $N = 107$. It follows that the iterative method based on the four-segment piecewise linear function could ensure the convergence to a rather accurate solution (with less than 5% error in linear parameter estimates) for a very high degree of nonlinearity, as indicated by the arrow in Figure 9b. The iterative method based on a polynomial of degree 4, on the other hand, can deal only with a moderate degree of nonlinearity. Voros's Wiener method, however, would fail unless the degree of nonlinearity is pretty low.

Another issue regarding the adequacy of least-squares solutions given by the two-stage algorithm is the effects of

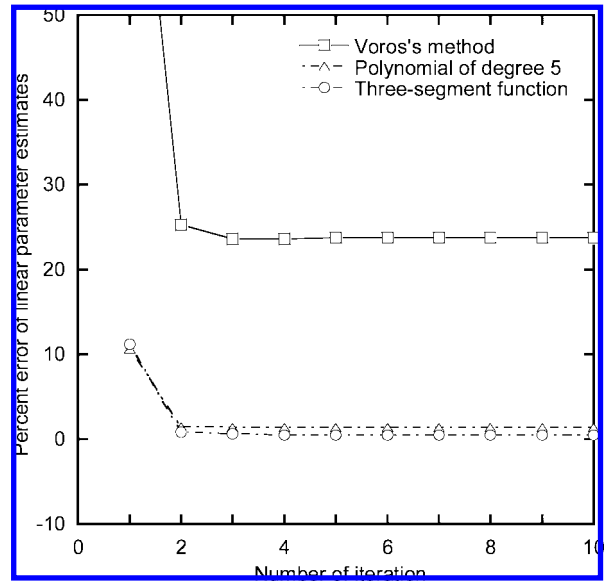

Figure 5. Convergence and accuracy properties of various iterative approaches for Example 1 with the type I static nonlinearity.

multicollinearity.[31] Multicollinearity means that two or more predictor variables in a multiple regression equation are highly correlated, so that the parameter estimates may change erratically in response to small changes in the equation or the data. A regression equation with multicollinearity can still provide a reliable model as a whole, but it may not give accurate estimation about each individual parameter. The variance inflation factor (VIF) is a good method of detecting the severity of multicollinearity.[31] Tables 1 and 2 list the VIF calculations for the algorithm applied to the Hammerstein Example 1 and the Wiener Example 2 in terms of the mean and the maximum of VIF factors, $\overline{\text{VIF}}$ and $\text{VIF}_{\max}$. It can be seen that for all cases, the first stage estimation is confronted by the severe problem of multicollinearity as revealed by very large values of $\overline{\text{VIF}}$ and $\text{VIF}_{\max}$. Consequently, the parameters of the linear dynamic part estimated at stage 1 vary considerably with the number of predictor variables (changes in the equation) and with the settings of η, λ, and N (changes in the data). Nevertheless, the estimated model as a whole is still reliable in approximating the static nonlinearity for each case as delineated in Figures 4 and 7. On the contrary, the values of $\overline{\text{VIF}}$ and $\text{VIF}_{\max}$ become very small for the second stage estimation. The accurate parameter estimates at stage 2 given in Tables 1 and 2 verify that the second stage estimation is indeed advantageous to recover the accuracy of the linear dynamic part.

In subsequent work, we consider the identification of three simulated physical examples and one experimental example that were discussed in literature. The two pH processes are essentially of Wiener type, whereas the simulated reactor process and the experimental heat exchanger are neither Hammerstein nor Wiener type. However, our iterative method can provide good Hammerstein or Wiener models for all four processes. All operating conditions are listed in Table 3.

Example 3. Consider a pH neutralization process employed by Nahas et al.[32] Acid, buffer, and base streams are mixed in a tank and the effluent pH is measured. This simulated physical process involves three nonlinear ordinary differential equations and a nonlinear algebraic equation for the pH:

$$\frac{dh}{dt} = \frac{1}{A}(q_1 + q_2 + q_3 - R_v h^{0.5})$$

Table 2. Two-Stage Estimation Results of Example 2 with the Type III Static Nonlinearity

		a_3	a_2	a_1	b_1	b_0	$\overline{\text{VIF}}$	$\text{VIF}_{\max}$
case D ($\eta = 15$, $\lambda = 0.1$, $N = 68$, $y_1 = 1.03$, $y_{-1} = -0.11$)	stage 1	0	5.171	3.705	−4.216	2.025	149.6	421.1
	stage 2	1.586	4.852	3.874	−4.331	2.025	2.07	2.80
case E ($\eta = 15$, $\lambda = 0.1$, $N = 68$, $y_1 = 1.01$, $y_{-1} = -0.09$)	stage 1	2.595	5.314	4.063	−3.693	1.932	124.7	359.5
	stage 2	1.970	4.929	3.985	−3.960	1.932	2.05	2.79
case F ($\eta = 12$, $\lambda = 0.05$, $N = 175$, $y_1 = 1.01$, $y_{-1} = -0.09$)	stage 1	2.908	5.611	4.039	−3.608	2.080	27.48	68.23
	stage 2	1.950	4.989	3.980	−4.216	2.080	2.37	3.32
case G ($\eta = 18$, $\lambda = 0.2$, $N = 27$, $y_1 = 1.01$, $y_{-1} = -0.09$)	stage 1	7.553	7.534	4.495	−2.441	2.169	39.07	98.75
	stage 2	2.128	4.901	4.075	−4.447	2.169	2.21	3.05

$$\frac{dW_{a4}}{dt} = \frac{1}{Ah}[(W_{a1} - W_{a4})q_1 + (W_{a2} - W_{a4})q_2 + (W_{a3} - W_{a4})q_3]$$

$$\frac{dW_{b4}}{dt} = \frac{1}{Ah}[(W_{b1} - W_{b4})q_1 + (W_{b2} - W_{b4})q_2 + (W_{b3} - W_{b4})q_3]$$

$$W_{a4} + 10^{pH-14} + W_{b4}\frac{1 + 2\times 10^{pH-pK_2}}{1 + 10^{pK_1-pH} + 10^{pH-pK_2}} - 10^{-pH} = 0$$

To identify this buffering pH process at the steady state of ($\bar{q}_3$, $\overline{\text{pH}}$) = (15.6 mL/s, 7.026), a white random input of the base flow q_3 with $T_s = 25$ and $\sigma = 25$ was employed and the pH was measured with NSR = 5%. The input q_3 was limited between 0 and 40 mL/s. Assuming the linear structure of $n = 1$, $m = 0$, and $d = 0$, the proposed two-stage algorithm with the four-segment piecewise linear function is applied to identify a Wiener model. The first stage of the algorithm with $\eta = 260$, $\lambda = 0.1$, and $N = 65$ provides a good piecewise linear fit to the static titration curve by plotting $y(t) + \overline{\text{pH}}$ versus $x(t)/\hat{b}_0 + \bar{q}_3$ according to eq 13 in Figure 10a. Figure 10b shows the fast convergence of the linear parameter estimates. The second stage of the algorithm with $\eta = 254$ confirms the assumed linear structure and gives rise to the linear dynamic element as

$$88.26x^{(1)}(t) + x(t) = 1.11u(t)$$

This estimate of the process time constant approximates closely the theoretical value of $A\bar{h}/(q_1 + q_2 + \bar{q}_3) = 88.49$. Such an agreement justifies that the pH process is indeed of Wiener type.

Note that it is not possible to describe perfectly the actual titration curve by the proposed four-segment function. However, our algorithm allows the linear dynamic part to be identified pretty well at the second stage insofar as the major trend of the static nonlinearity can be captured. The identified linear part given above could arrive at a fairly good estimate of the internal variable, $\hat{x}_{lin}(t)$. As a result, in the plot of $y(t) + \overline{\text{pH}}$ versus $\hat{x}_{lin}(t)/\hat{b}_0 + \bar{q}_3$, numerous data points can be observed to fluctuate around the actual titration curve as evidenced in the subplot of Figure 10a. We then propose a simple data smoothing technique to provide a perfect fit to the titration curve as follows. First divide the observed data points into a number of neighboring clusters. Next determine each smoothed data point by averaging

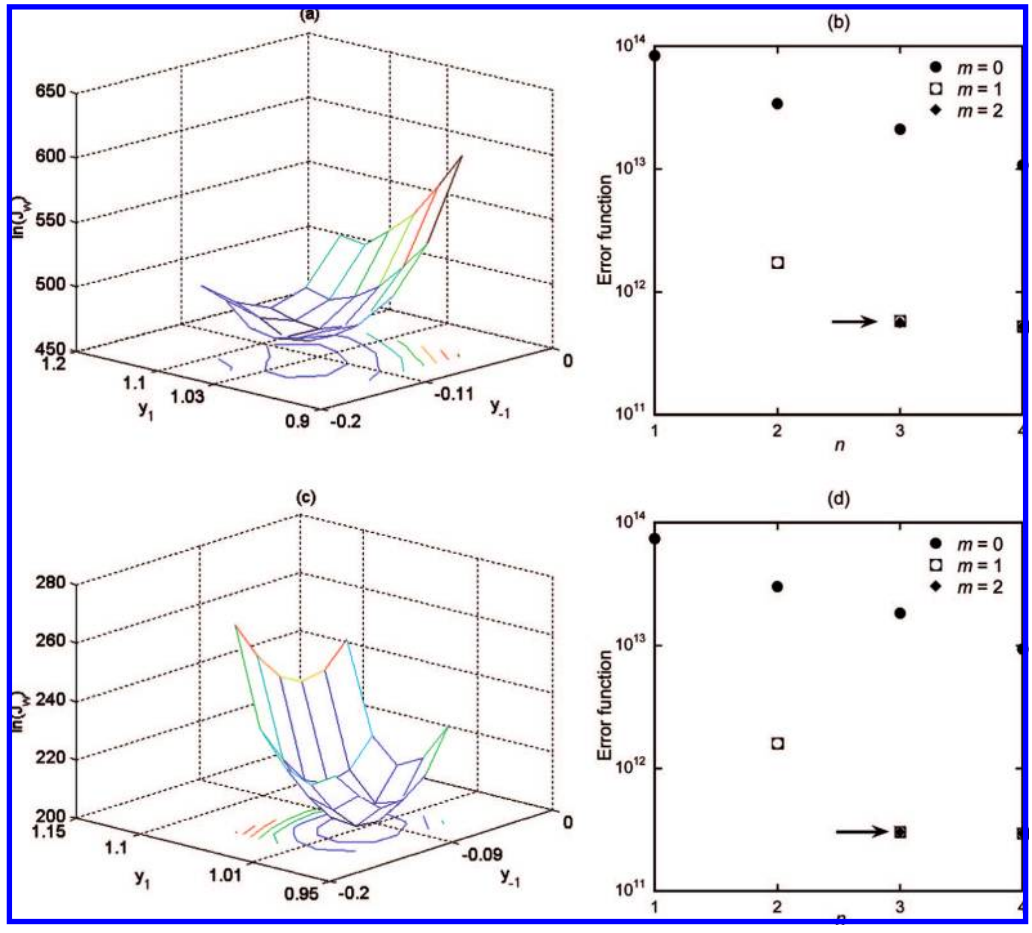

Figure 6. Determination of the partition points and linear structure for Wiener identification of Example 2 with the type III static nonlinearity: (a, b) case D; (c, d) case E.

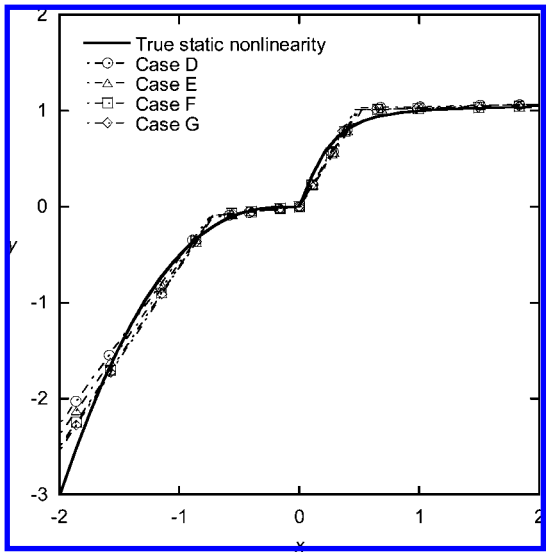

Figure 7. Approximations of the type III static nonlinearity by Wiener identification of Example 2.

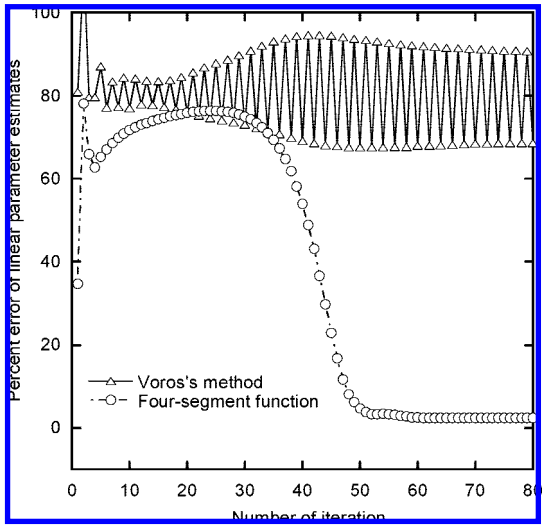

Figure 8. Convergence properties of two iterative approaches for Wiener identification of Example 2 with the type III static nonlinearity.

the original data points contained within each cluster. Figure 10a verifies that the titration curve can indeed be constructed perfectly by the smoothed data points.

Example 4. Another pH process, discussed by Palancar et al.,[25] involves the neutralization of acetic acid (AcH), propionic acid (PrH), and sodium hydroxide (NaOH) in a single tank. Without buffering, this physical process exhibits a high degree of nonlinearity and can be simulated as

$$\frac{dC_{AcH}}{dt} = \frac{1}{V}[q_a C_{0AcH} - (q_a + q_b)C_{AcH}]$$

$$\frac{dC_{PrH}}{dt} = \frac{1}{V}[q_a C_{0PrH} - (q_a + q_b)C_{PrH}]$$

$$\frac{dC_{NaOH}}{dt} = \frac{1}{V}[q_b C_{0NaOH} - (q_a + q_b)C_{NaOH}]$$

$$\frac{C_{AcH}}{1 + 10^{pK_{AcH} - pH}} + \frac{C_{PrH}}{1 + 10^{pK_{PrH} - pH}} + 10^{pH-14} - C_{NaOH} - 10^{-pH} = 0$$

where q_a and q_b are the flow rates of acidic and alkaline streams,

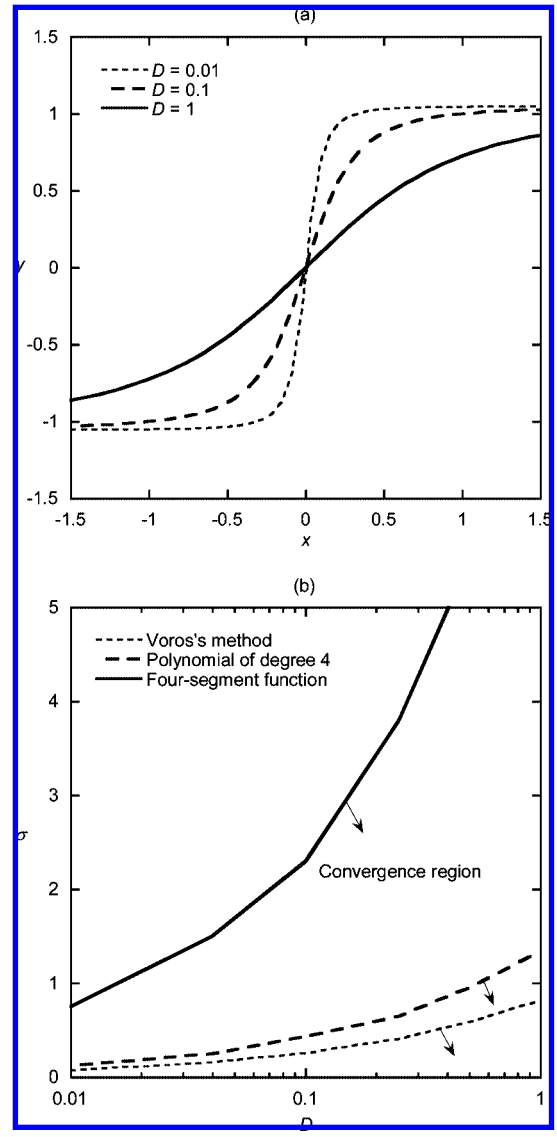

Figure 9. Convergence analysis of various iterative approaches based on the Wiener Example 2 with the type IV static nonlinearity: (a) degree of static nonlinearity; (b) range of test input for convergence.

V is the tank volume, and C denotes the concentration. For the sake of identification, a white random signal with $T_s = 0.01$ and $\sigma = 5$ was introduce to the base flow q_b and the resulting pH was measured with NSR = 5%. The input q_b was limited between 5 and 25 mL/s. Assuming $n = 1$, $m = 0$, and $d = 0$, the proposed two-stage algorithm with the four-segment piecewise linear function is applied to identify three Wiener models corresponding to arbitrarily selected steady states of ($\bar{q}_b$, $\overline{pH}$) = (13.5 mL/s, 6.099), (14.2 mL/s, 9.407), (15 mL/s, 12.739). Note that these steady states are located widely apart along the static titration curve as seen in Figure 11a. The first stage of the algorithm with $\eta = 0.15$, $\lambda = 0.1$, and $N = 65$ gives similar piecewise linear fits to the static titration curve by plotting $y(t) + \overline{pH}$ against $x(t)/\hat{b}_0 + \bar{q}_b$ according to eq 13 in Figure 11a, while the second stage of the algorithm with $\eta = 0.1$ confirms the assumed linear structure and identifies three linear dynamic elements as

$$0.0370x^{(1)}(t) + x(t) = 4.693u(t) \qquad \text{for } \bar{q}_b = 13.5$$

$$0.0354x^{(1)}(t) + x(t) = 6.706u(t) \qquad \text{for } \bar{q}_b = 14.2$$

$$0.0363x^{(1)}(t) + x(t) = 0.3738u(t) \qquad \text{for } \bar{q}_b = 15$$

Table 3. Nominal Operating Conditions for Simulated and Experimental Examples

Example 3	$A = 207$ cm^2, $R_v = 8.75$ mL/cm/s, p$K_1 = 6.35$, p$K_2 = 10.25$, $W_{a1} = 3\times10^{-3}$ M, $W_{a2} = -3\times10^{-2}$ M, $W_{a3} = -3.05\times10^{-3}$ M, $W_{b1} = 0$, $W_{b2} = 3\times10^{-2}$ M, $W_{b3} = 5\times10^{-5}$ M, $q_1 = 16.6$ mL/s, $q_2 = 0.55$ mL/s
Example 4	$q_a = 14.2$ mL/s, $V = 1.0$ L, $C_{0AcH} = 1$ M, $C_{0PrH} = 1$ M, $C_{0NaOH} = 2$ M, p$K_{AcH} = 4.75$, p$K_{PrH} = 4.87$
Example 5	$C_{Af} = 10$ M, $V = 1.0$ L, $k_1 = 50$ h^{-1}, $k_2 = 100$ h^{-1}, $k_3 = 10$ M^{-1} h^{-1}
Example 6	inlet water temperature = 30 °C, process water exit temperature = 62.5 °C, process water flow rate = 42% of maximum (1.12 volt$^{1/2}$), steam flow rate = 62% of maximum

It is interesting to note that the two-stage algorithm yields consistent estimation results for the linear dynamic part despite appreciable fitting errors given by the four-segment function in the middle (steep) region of the titration curve. Note also that the three estimates of the process time constant approximate closely the theoretical values of $V/(q_a + \bar{q}_b) \cong 0.0361\sim0.0342$. Applying the preceding data smoothing technique to the data points created by plotting $y(t) + \overline{\text{pH}}$ versus $\hat{x}_{lin}(t)/\hat{b}_0 + \bar{q}_b$, resulting from any of the above three linear parts, could establish a perfect fit to the titration curve as elaborated in Figure 11a. The effectiveness of the identified Wiener models is further verified by the agreement between the predicted output and the actual response caused by step-input changes in Figure 11b.

Example 5. Harris et al.[33] and Jia et al.[28] considered the Van de Vusse reactions, A→B→C and 2A→D, which were carried out in an isothermal continuous stirred-tank reactor. The dynamics of the reactor process can be simulated by

$$\frac{dC_A}{dt} = -k_1 C_A - k_3 C_A^2 + \frac{F}{V}(C_{Af} - C_A)$$

$$\frac{dC_B}{dt} = k_1 C_A - k_2 C_B - \frac{F}{V} C_B$$

Notably, C_B is the effluent concentration of component B and

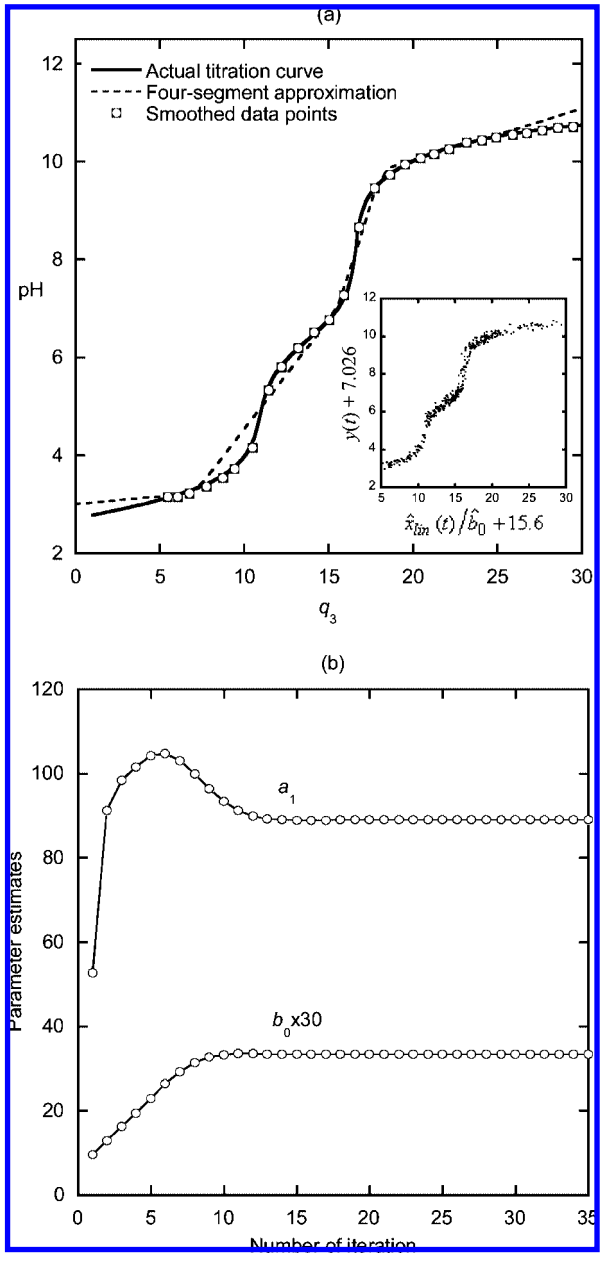

Figure 10. Identification results of Example 3: (a) approximations of the titration curve; (b) convergence of the linear parameter estimates.

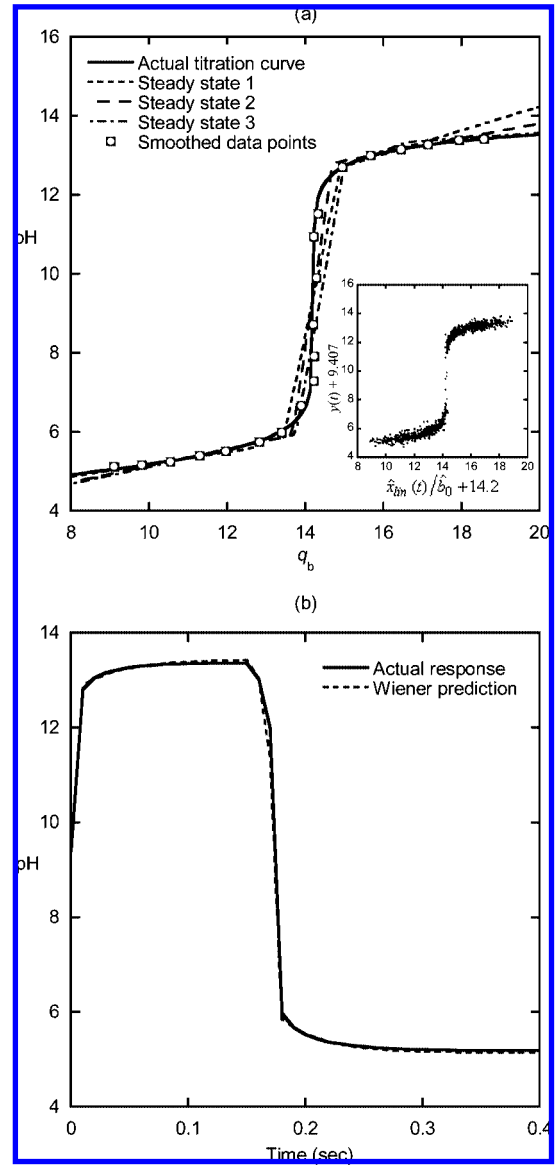

Figure 11. Identification results of Example 4: (a) approximations of the titration curve; (b) comparison of model predictions with the actual response caused by step-input changes.

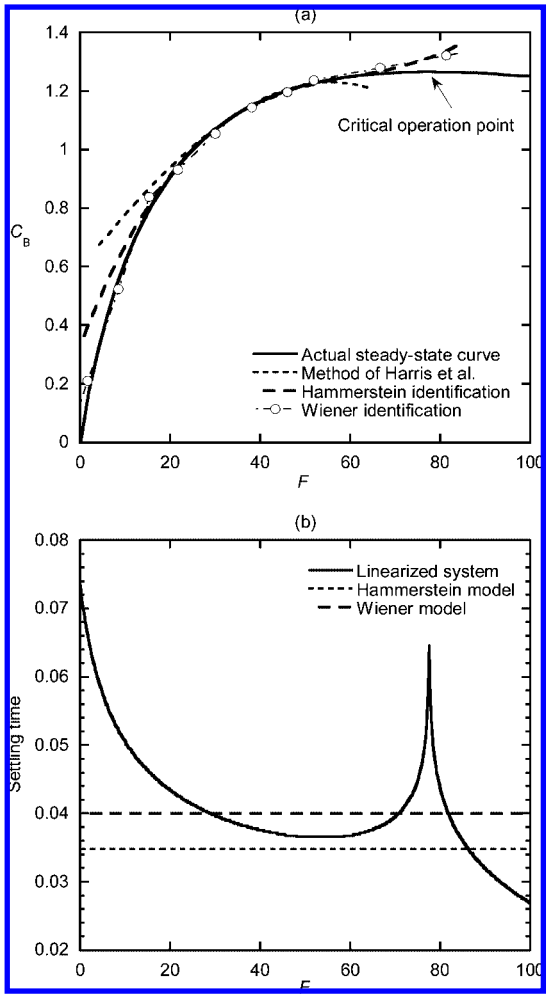

Figure 12. Identification results of Example 5: (a) approximations of the steady-state curve; (b) variations in the settling time of the linearized system as well as Hammerstein and Wiener estimates.

F is the inlet flow rate. The concentration measurement is assumed to be delayed by 0.02 h. The process is nonlinear as evidenced by the actual steady-state curve given in Figure 12a. However, it is neither Hammerstein nor Wiener because the dynamics linearized at different steady-state operation points exhibit widely distinct characteristics as seen in Figure 12b, which depicts variations in the settling time of the linearized system. Moreover, both the steady-state gain and dynamic zero alter from positive to negative at the operation point of $F = 77.5$ L/h. This implies that identification involving this critical operation point is difficult in that a portion of static nonlinearity would become noninvertible and a drastic change from inverse response to overshoot would be encountered.

To identify the process at the steady state of $(\bar{F}, \bar{C}_B) = (34.3$ L/h, 1.117 M), a white random sequence with $T_s = 0.02$ and $\sigma = 30$ was introduced to the input flow rate F, and the output concentration C_B was measured with NSR = 5%. The input F was limited between 0 and 100 L/h. Assuming the linear structure of $n = 2$, $m = 1$, and $d = 0.02$, the proposed two-stage algorithm is applied to identify a Wiener model with the four-segment piecewise linear function. The first stage of the algorithm converges in 11 iteration steps using the parameters of $\eta = 0.1$, $\lambda = 0.1$, and $N = 80$. The resulting four-segment piecewise linear function provides a good fit to the entire steady-state curve except for the region near the critical operation point as shown in Figure 12a. This exception is not surprising because this critical region violates the invertible condition stipulated

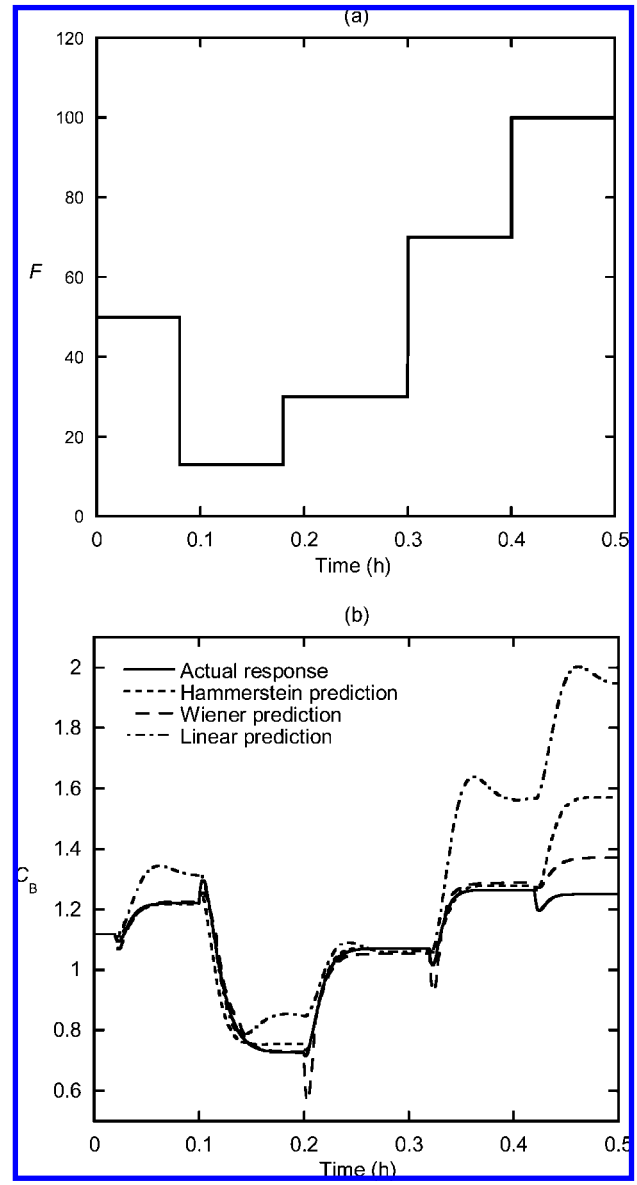

Figure 13. Model validation of Example 5: (a) applied input signal; (b) model predictions versus the actual response.

by the four-segment function for static nonlinearity. The second stage of the algorithm with $\eta = 0.05$ confirms the assumed linear structure and gives rise to the linear dynamic element as

$$5.18\times10^{-5}x^{(2)}(t) + 1.46\times10^{-2}x^{(1)}(t) + x(t) = -4.91\times10^{-5}u^{(1)}(t-0.02) + 6.80\times10^{-3}u(t-0.02)$$

This estimation of the linear dynamic part leads to a constant settling time of 0.04 h (ignoring the time delay). Figure 12b reveals that the dynamic part of the Wiener model converges to an "average" linear model that approximates the variable nonlinear dynamics as closely as possible.

Our algorithm can also identify the process as a Hammerstein model with a polynomial of degree 3. The second stage of the algorithm with $\eta = 0.025$ gives rise to the linear dynamic element as

$$6.67\times10^{-5}y^{(2)}(t) + 1.45\times10^{-2}y^{(1)}(t) + y(t) = -3.50\times10^{-3}x^{(1)}(t-0.02) + x(t-0.02)$$

Figure 12 indicates that the estimation of the nonlinear static and linear dynamic parts by Hammerstein identification is less

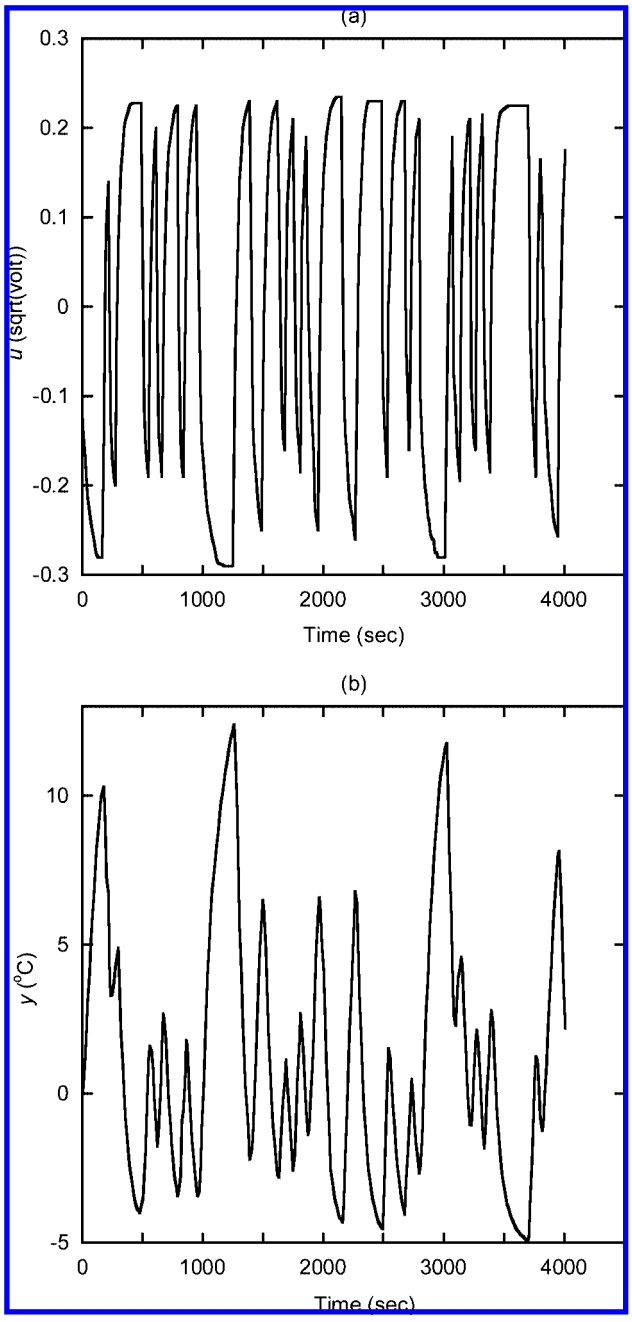

Figure 14. Experimental input−output data of the heat exchanger example obtained from Eskinat et al.[34]

accurate than that given by Wiener identification. Figure 12a also compares the steady-state curve obtained by the method of Harris et al.[33] It can be seen that the model of Harris et al. is valid only for a narrow operating range.

For model validation, we apply a stepwise input signal that covers a wide operating range as seen in Figure 13a. Figure 13b compares the actual response against those predicted by the Hammerstein and Wiener models as well as a linear model, estimated by the method of Hwang and Lin. It appears that both the Hammerstein and Wiener models describe the nonlinear system reasonably well and are far superior to the linear model. It is worth mentioning that the Hammerstein model as a whole is good though the estimated static and dynamic parts are less accurate. Inevitably, all the models, characterized by positive steady-state gains and inverse response, fail during the final period of response where the input F is changed from 70 to 100 L/h. Recall that for this particular operating region, the actual response experiences an appreciable overshoot and the steady-state gain becomes negative.

Example 6. In addition to the preceding simulated examples, we apply the proposed method to the experimental data of a real steam-water heat exchanger acquired by Eskinat et al.[34] In their experimental setup, the steam condensed in a two-pass shell and tube heat exchanger, thereby raising the process water temperature. The steam flow rate and process water flow rate were controlled by pneumatic control valves. A PRBS identification test with a switching time of 1 min was performed on the heat exchanger in closed-loop operation. The water flow rate was changed by varying the setpoint of the controller, keeping the steam flow constant. The measurements of the process water exit temperature were fed to a data acquisition system with a sampling time of 12 seconds. The experimental

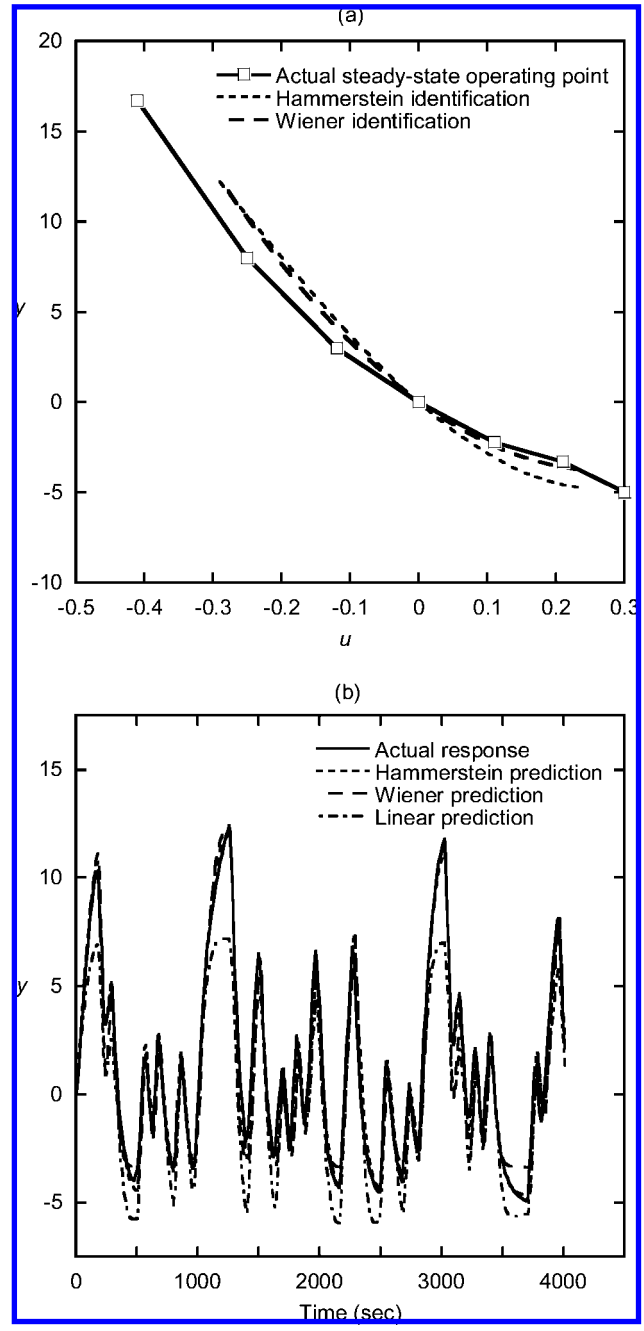

Figure 15. Identification (before $t = 3000$ sec) and model validation (after $t = 3000$ sec) results of Example 6: (a) fitted static behaviors and actual steady-state data from Eskinat et al.;[34] (b) model predictions versus actual response data.

input−output data are plotted in Figure 14, where the deviation variables u and y denote, respectively, changes in the water flow rate and changes in the water exit temperature. They also provided steady-state operation data as shown in Figure 15a.

The two-stage algorithm, assuming $\eta = 144$, $n = 2$, $m = 1$, and $d = 0$ for the first stage, can identify the process as a Hammerstein model with a polynomial of degree 3 and a Wiener model with a polynomial of degree 2 based on the training input−output data during the period of $0 \le t \le 3000$ seconds. The rest of the data is used to test the validity of the identified models. It should be mentioned that the selected η value was obtained by trying different values for η until rather consistent solutions appeared. The Hammerstein model is estimated as

$$154.1y^{(2)}(t) + 54.84y^{(1)}(t) + y(t) = -0.7825x^{(1)}(t) + x(t)$$

$$x(t) = -33.30[u(t)] + 44.47[u(t)]^2 + 48.01[u(t)]^3$$

while the Wiener model is estimated as

$$88.98x^{(2)}(t) + 42.58x^{(1)}(t) + x(t) = 204.3u^{(1)}(t) - 27.30u(t)$$

$$y(t) = x(t) + 0.0736[x(t)]^2$$

The estimated static nonlinearities are compared to the steady-state operation data in Figure 15a. The two nonlinear models follow the trend in the operation data closely. The simulated responses of the Hammerstein and Wiener models are compared with the actual response in Figure 15b. It can be seen that both models fit the actual response data very well. A close examination reveals that the Wiener model is better in approximating the static nonlinearity, while the Hammerstein model is better in estimating the nonlinear dynamic response. On the contrary, the linear model, estimated using the method of Hwang and Lin, results in a considerable discrepancy in the linear and the actual responses.

7. Conclusions

It has been demonstrated that the proposed iterative method could identify effectively SISO Hammerstein or Wiener models for a variety of nonlinear process dynamics and test conditions. The method incorporates two mechanisms, moving-horizon smoothing and solution-guiding, to facilitate the convergence and accuracy of the iteration procedure. The method deals successfully with the situations of linear structure mismatch, high static nonlinearity with an unknown characteristic, a wide range of test data, and severe measurement noise. Under such situations, the two-stage estimation algorithm can ensure the adequacy of both the nonlinear and linear parts in a sequential manner. Moreover, the two-stage algorithm is not sensitive to the prior assumption of the linear structure and the first stage settings of η, λ, and N.

The proposed method approximates the static nonlinearity by a polynomial or a multisegment function. The assumption of such functions would limit the practical application of the method when the actual nonlinear static behavior is very different from the assumed form or is invertible in some operating region. Nevertheless, several simulated examples indicate that the proposed method could arrive at good estimation of the linear dynamic part insofar as the assumed function could catch the major trend in the static nonlinearity. For Wiener identification, the data smoothing technique can be employed to provide a more accurate description about the nonlinear static behavior.

If the process is neither Hammerstein nor Wiener type, the proposed method is still suited to identifying it as a Hammerstein or Wiener model. The resultant model is quite useful to the controller design of the nonlinear process. Note that all four physical examples (simulated or experimental) can be described by the identified Wiener models reasonably well. This agrees with the claim of Boyd and Chua.[11]

Acknowledgment

This work was supported by the National Science Council of R.O.C. under Grant NSC 97-2221-E-006-171. Thanks are given to the anonymous reviewer for helpful comments.

Nomenclature

A = cross-sectional area
a_i = model parameters of the linear part in a Hammerstein or Wiener model
b_i = model parameters of the linear part in a Hammerstein or Wiener model
C_i = concentration of species i
c_i = model parameters of the nonlinear part in a Hammerstein or Wiener model
D = constant defined in Example 2
d = time delay
e_i = model parameters of the nonlinear part described by a four-segment function
F = inlet flow rate
f = continuous-time signal
f_i = function formed by $h_i[u(t)]$
g_i = function formed by $h_i[y(t)]$
h = liquid level
$h_i[\cdot]$ = switching function
J = error criterion
k = number of regression relations or the iteration step
k_i = reaction rate constant
L^{-1} = inverse Laplace transform
m = system order
N = total number of regression relations
n = system order
p = degree of a polynomial
pK_i = log of equilibrium constant for i
q_i = volumetric flow rate
R_v = valve coefficient
$T_l\{\cdot\}$ = lth-order integral transform
T_s = switching time of a test input
t = time
t_i = time instant denoted by i
$U(s)$ = Laplace transform of $u(t)$
u = input variable
$u_{\pm 1}$ = partition points for the three-segment function
V = volume of liquid in the tank
W_i = reaction invariant i
w = weighting function
x = internal variable
y = output variable
$y_{\pm 1}$ = partition points for the four-segment function

Greek Symbols

$\boldsymbol{\varphi}$ = regression vector
η = horizon length
λ = argument defined in eq 24
$\boldsymbol{\theta}$ = parameter vector
σ = standard deviation

Superscripts

(j) = jth derivative with respect to time
T = transpose of a vector

Subscripts

h = Hammerstein
L = lower bound
lin = linear dynamic block
M = model predicted
nl = nonlinear static block
U = upper bound
w = Wiener

Literature Cited

(1) Ljung, L. *System Identification: Theory for the User*; Prentice Hall: Upper Saddle River, NJ, 1999.

(2) Hwang, S. H.; Lin, M. L. Unbiased Identification of Continuous Time Parametric Models Using a Time-Weighted Integral Transform. *Chem. Eng. Commun.* **2003**, *190*, 1170.

(3) Haber, R.; Unbehauen, H. Structure Identification of Nonlinear Dynamic Systems-A Survey on Input/Output Approaches. *Automatica* **1990**, *26*, 651.

(4) Bloemen, H. H. J.; Chou, C. T.; van den Boon, T. J. J.; Verdult, V.; Verhaegen, M.; Backx, T. C. Wiener Model Identification and Predictive Control for Dual Composition Control of a Distillation Column. *J. Process Control* **2001**, *11*, 601.

(5) Singh, M. G.; Elloy, J. P.; Mezencev, R.; Munro, N. *Applied Industrial Control*; Pergamon Press: Oxford, U.K., 1980.

(6) Kalafatis, A.; Arifin, N.; Wang, L.; Cluett, W. R. A New Approach to the Identification of pH Processes Based on the Wiener Model. *Chem. Eng. Sci.* **1995**, *50*, 3693.

(7) Norquary, S. J.; Palazoglu, A.; Romagnoli, J. A. Model Predictive Control Based on Wiener Models. *Chem. Eng. Sci.* **1998**, *53*, 75.

(8) Fruzzetti, K. P.; Palazoglu, A.; McDonald, K. A. Nonlinear Model Predictive Control Using Hammerstein Models. *J. Process Control* **1997**, *7*, 31.

(9) Huang, H. P.; Lee, M. W.; Tang, Y. T. Identification of Wiener Model Using Relay Feedback Test. *J. Chem. Eng. Jpn.* **1998**, *31*, 604.

(10) Lee, M. W.; Huang, H. P. Identification and Control of Hammerstein-Type Nonlinear Process. *J. Chin. Inst. Chem. Eng.* **2001**, *32*, 361.

(11) Boyd, S.; Chua, L. O. Fading Memory and the Problem of Approximating Nonlinear Operators with Volterra Series. *IEEE Trans. Circuits Syst.* **1985**, *CAS-32*, 1150.

(12) Greblicki, W.; Pawlak, M. Identification of Discrete Hammerstein Systems Using Kernel Regression Estimates. *IEEE Trans. Autom. Control* **1986**, *AC-31*, 74.

(13) Greblicki, W.; Pawlak, M. Nonparametric Identification of Hammerstein Systems. *IEEE Trans. Inf. Theory* **1989**, *IT-35*, 409.

(14) Lang, Z. Q. A Nonparametric Polynomial Identification Algorithm for the Hammerstein System. *IEEE Trans. Autom. Control* **1997**, *AC-42*, 1435.

(15) Narenda, K. S.; Gallman, P. G. An Iterative Method for the Identification of Nonlinear Systems Using the Hammerstein Model. *IEEE Trans. Autom. Control* **1966**, *AC-11*, 546.

(16) Chang, F. H. I.; Luss, R. A Noniterative Method for Identification Using Hammerstein Model. *IEEE Trans. Autom. Control* **1971**, *AC-16*, 464.

(17) Voros, J. Iterative Algorithm for Parameter Identification of Hammerstein System with Two-Segment Nonlinearities. *IEEE Trans. Autom. Control* **1999**, *44*, 2145.

(18) Voros, J. Modeling and Identification of Wiener Systems with Two-Segment Nonlinearities. *IEEE Trans. Controlled Syst. Technol.* **2003**, *11*, 253.

(19) Pajunen, G. A. Adaptive Control of Wiener Type Nonlinear Systems. *Automatica* **1992**, *28*, 781.

(20) Wigren, T. Recursive Prediction Error Identification Using the Nonlinear Wiener Model. *Automatica* **1993**, *29*, 1011.

(21) Van Pelt, T. H.; Bernstein, D. S. Non-Linear System Identification Using Hammerstein and Non-linear Feedback Models with Piecewise Linear Static Maps. *Int. J. Control* **2001**, *74*, 1807.

(22) Voros, J. Parameter Identification of Wiener Systems with Multisegment Piecewise-Linear Nonlinearities. *Syst. Control Lett.* **2007**, *56*, 99.

(23) Su, H.; McAvoy, T. J. Integration of Multilayer Perception Networks and Linear Dynamic Models: A Hammerstein Modeling Approach. *Ind. Eng. Chem. Res.* **1993**, *32*, 1927.

(24) Al-Duwaish, H.; Karim, M. N. A New Method for the Identification of Hammerstein Model. *Automatica* **1997**, *33*, 1871.

(25) Palancar, M. C.; Aragon, J. M.; Torrecilla, J. S. pH-Control Systems Based on Artificial Neural Networks. *Ind. Eng. Chem. Res.* **1998**, *37*, 2729.

(26) Sung, S. W. System Identification Method for Hammerstein Processes. *Ind. Eng. Chem. Res.* **2002**, *41*, 4295.

(27) Bai, E. W. Decoupling the Linear and Nonlinear Parts in Hammerstein Model Identification. *Automatica* **2004**, *40*, 671.

(28) Jia, L.; Chiu, M. S.; Ge, S. S. A Noniterative Neuro-Fuzzy Based Identification Method for Hammerstein Processes. *J. Process Control* **2005**, *15*, 749.

(29) Chen, H. F. Pathwise Convergence of Recursive Identification Algorithms for Hammerstein Systems. *IEEE Trans. Autom. Control* **2004**, *49*, 1641.

(30) Hu, X. L.; Chen, H. F. Strong Consistence of Recursive Identification for Wiener Systems. *Automatica* **2005**, *41*, 1905.

(31) Neter, J.; Wasserman, W.; Kutner, M. H. *Applied Linear Regression Models*, 2nd ed.; Richard, D., Ed.; Irwin: Homewood, Il, 1989.

(32) Nahas, E. P.; Henson, M. A.; Seborg, D. E. Nonlinear Internal Model Control Strategy for Neural Network Models. *Comput. Chem. Eng.* **1992**, *16*, 1992.

(33) Harris, K. R.; Colantonio, M. C.; Palazoglu, A. On the Computation of a Nonlinearity Measure Using Functional Expansions. *Chem. Eng. Sci.* **2000**, *55*, 2393.

(34) Eskinat, E.; Johnson, S. H.; Luyben, W. L. Use of Hammerstein Models in Identification of Nonlinear Systems. *AIChE J.* **1991**, *37*, 255.

Received for review January 28, 2008
Revised manuscript received October 18, 2008
Accepted October 21, 2008

IE800149W